Biasymptotic formula for the turbulent energy cascade

R. Badii* and P. Talkner
General Energy Research Department, Paul Scherrer Institute, 5232 Villigen, Switzerland
(Received 1 June 1999)

We present a family of differential models for the scaling exponents τ_p which characterize the moments of the energy dissipation rate in turbulence. This scheme interpolates between the asymptotic values of the derivative τ_p' of τ_p versus p in the limits $p \to \pm\infty$ and reproduces the negative-p part of the exponents spectrum τ_p as well, in contrast with other recent conjectures. Each member of the family is defined by a sigmoidal function, the form of which remains open to theoretical investigations. [S1063-651X(99)10510-5]

PACS number(s): 47.27.Gs, 02.50.−r, 05.40.−a

I. INTRODUCTION

One of the most striking features of turbulent flows at high Reynolds number is the apparent universality of small-scale velocity fluctuations, for which the effects of the boundary conditions can be neglected. In particular, the moments of suitable observables characterizing spatial domains of size ℓ present a power-law dependence on ℓ, with universal exponents. This is expected to hold in the so-called *inertial range* $\ell_{\min} \ll \ell \ll \ell_{\max}$, where $\ell_{\max}$ is the energy-injection scale and $\ell_{\min}$ is the length below which dissipation prevails. For example, the moments of the longitudinal velocity difference $d(\ell) = [\boldsymbol{v}(\boldsymbol{x}+\boldsymbol{\ell},t) - \boldsymbol{v}(\boldsymbol{x},t)] \cdot \boldsymbol{\ell}/\ell$, where $\boldsymbol{v}(\boldsymbol{x},t)$ is the velocity field of the fluid at the space-time point $(\boldsymbol{x},t)$ and $\boldsymbol{\ell}$ is a displacement vector of length ℓ, are expressed as

$$S_p(\ell) \equiv \langle d^p(\ell) \rangle \sim \ell^{\zeta_p}. \tag{1.1}$$

This behavior was first postulated by Kolmogorov [1] under the assumption that energy was passed from the large to the small scales without alteration in the inertial range (IR), so that the only relevant parameters for the statistics were ℓ and the mean energy dissipation rate $\langle \varepsilon(\ell) \rangle$, which is nearly ℓ independent. The local rate $\varepsilon(\ell)$ is defined as

$$\varepsilon(\ell) = \frac{2\nu}{|B|} \int_B \sum_{ij} S_{ij}(\boldsymbol{x}) S_{ji}(\boldsymbol{x}) dV, \tag{1.2}$$

where $B = B(\boldsymbol{x};\ell)$ is a domain centered at $\boldsymbol{x}$ and having volume $|B| \sim \ell^3$, $S_{ij} = (\partial v_i/\partial x_j + \partial v_j/\partial x_i)/2$ is the symmetric part of the strain rate tensor, and ν is the kinematic viscosity. Furthermore, Kolmogorov [1] proved the exact IR relation

$$\langle d^3(\ell) \rangle \sim -\frac{4}{5} \ell \langle \varepsilon(\ell) \rangle \tag{1.3}$$

and applied dimensional considerations to the Navier-Stokes equations [2] obtaining the prediction $\zeta_p = p/3$ (K41).

Deviations of the experimental estimates of ζ_p from this value and theoretical objections led to the formulation of a refined hypothesis (K62) [3,4] which assumed Eq. (1.3) to be a particular case of the more general relation

$$\langle d^p(\ell) \rangle \sim \ell^{p/3} \langle \varepsilon^{p/3}(\ell) \rangle \tag{1.4}$$

which links the fluctuations of the velocity field with those of the dissipation field. By defining energy dissipation exponents τ_p via the moments

$$M_p(\ell) \equiv \langle \varepsilon^p(\ell) \rangle \sim \ell^{\tau_p}, \tag{1.5}$$

this link is finally expressed by

$$\zeta_p = p/3 + \tau_{p/3}. \tag{1.6}$$

Experiments show that the exponents τ_p deviate considerably from zero, especially for large $|p|$ [5–7]. The refined K62 approach, under the assumption of a lognormal statistics for the variable $\varepsilon(\ell)$, yields the expression

$$\tau_p^{(\mathrm{K62})} = -\tau_2 p(1-p)/2, \tag{1.7}$$

where $\tau_2 \approx -0.18$ [5–8]. While Eq. (1.7) provides a good fit to the data for $0 \leq p \leq 2$, the parabolic falloff of the curve is too steep.

Since direct estimates of τ_p for large $|p|$ are statistically unreliable and our physical understanding of turbulent fluctuations is not sufficient to yield the form of the function τ_p, even up to unknown parameters, simple analytical approximations to τ_p have been attempted. The underlying assumptions essentially fall into three classes: in the first, the energy cascade is viewed as a multiplicative stochastic process [9–14]; in the second, assumptions are made about the distribution of the "breakdown coefficient" $\varepsilon(r\ell)/\varepsilon(\ell)$ [15,16] (where $0 < r < 1$); in the third, assumptions about the asymptotic behavior of τ_p for $p \to +\infty$ are combined with scaling laws which relate moments M_{p-1}, M_p, and M_{p+1} [Eq. (1.5)] with one another [17,18], rather than with the length scale ℓ.

In the present paper, we propose a differential reformulation of the latter approach which accounts for arbitrary increments to the order p (i.e., not just ± 1), modifies accordingly the asymptotic scaling assumption, and takes into account the limit $p \to -\infty$ as well. This goal is achieved by introducing a class of sigmoidal functions which control the shape (curvature) of the exponent τ_p versus p. Some yield

*URL: http://www1.psi.ch/~badii

better agreement with the experiment for $p \in (-1,3)$, some outside this range. As a result, the differences among various current approximations [16–19] and their relative degree of success can be easily assessed.

Since these are essentially phenomenological models, not based on any real physical understanding of the basic mechanisms of turbulence, our introduction of a whole class of model functions should not be dismissed as a mere technical artifact to achieve a fit but seen as a further confirmation that no physical criterion presently exists to discriminate between possible models. As already suggested in Ref. [19], it is unlikely that this goal may be achieved by experiment only. Indeed, all of the functions we consider provide good fits to the experimental estimates. The latter have been performed on different measurements of atmospheric turbulence with Reynolds-Taylor numbers around 10000, sampling rates between 2 and 30 kHz, spatial resolution of 2 mm, and 12-bit accuracy [7,8].

II. MODEL

Rather than studying the ℓ dependence of the moments $M_p(\ell)$ (1.5), She and Lévêque [17] have proposed to compare moments of different order p with one another at a fixed scale ℓ: in particular, they considered the ratio

$$Z_\ell(p,q) = M_p(\ell)/M_q(\ell) \sim \ell^{\tau_p - \tau_q} \tag{2.1}$$

for $q = p-1$ and postulated the relation

$$Z_\ell(p+1,p) = A_p Z_\ell^\beta(p,p-1) Z_\ell^{1-\beta}(\infty+1,\infty), \tag{2.2}$$

where A_p is independent of ℓ, β is a constant, and $Z_\ell(\infty+1,\infty) = \lim_{p\to\infty} Z_\ell(p+1,p)$. By inserting Eq. (1.5) into (2.2), assuming that $Z_\ell(\infty+1,\infty) \sim \ell^{-t_+}$, with $t_+ = 2/3$, and using the relations

$$\tau_0 = \tau_1 = 0, \tag{2.3}$$

She and Lévêque (SL) finally obtained

$$\tau_p^{(\mathrm{SL})} = -\frac{2}{3}p + 2\left[1 - \left(\frac{2}{3}\right)^p\right]. \tag{2.4}$$

Although this formula is close to the experimental findings, the choice $t_+ = 2/3$ has been criticized by Novikov [16], who proposed the value $t_+ = 1$: this has led to a numerical modification of the SL formula by Chen and Cao [18] which reads

$$\tau_p^{(\mathrm{CC})} = -p + [(1+\tau_2)^p - 1]/\tau_2. \tag{2.5}$$

While the latter is closer to the experimental results in the range $-0.5 \leqslant p \leqslant 5$, the former is slightly more accurate for $p > 5$ [7]. Moreover, both functions exhibit an exponential falloff for negative p which is in stark disagreement with the observation. This should not be surprising, since these models are based on a conjecture about the limit $p \to \infty$. Indeed, a linear behavior of τ_p seems to be correct, within the available precision, also for $p < 0$ [7]. Finally, the scaling law (2.2) is not well verified, especially for small $|p|$, where the increment by 1 in p is too large (a simpler and more accurate relation between moments has been illustrated in Ref. [7]).

Motivated by these inconsistencies, we first reformulate the SL approach using an arbitrary increment h for the moment's order p and later extend it by introducing a scaling exponent for $Z_\ell(p+h,p)$ in the limit $p \to -\infty$ as well. We rewrite Eq. (2.2) as

$$Z_\ell(p+h,p) \sim Z_\ell^{bh}(\infty+h,\infty) Z_\ell^{1-bh}(p,p-h), \tag{2.6}$$

where $Z_\ell(\infty+h,\infty) = \lim_{p\to\infty} Z_\ell(p+h,p)$, $b \geqslant 0$ is a constant and h is an arbitrary real increment. This equation clearly implies the vicinity of $Z_\ell(p+h,p)$ and $Z_\ell(p,p-h)$ (an identity for $h \to 0$) and attributes a "weight" to the asymptotic value $Z_\ell(\infty+h,\infty)$ which vanishes for $h \to 0$ [i.e., the first factor on the right-hand side (RHS) of Eq. (2.6) tends to 1]. Assuming

$$Z_\ell(\infty+h,\infty) \sim \ell^{-t_+ h} \tag{2.7}$$

and recalling Eq. (1.5) yields

$$\tau_{p+h} - \tau_p \approx -b t_+ h^2 + (1-bh)(\tau_p - \tau_{p-h}). \tag{2.8}$$

Subtracting $\tau_p - \tau_{p-h}$ from both sides, dividing by h^2, and taking the limit $h \to 0$ yields the differential equation

$$\tau_p'' \approx -b\tau_p' - bt_+, \tag{2.9}$$

where each prime denotes a derivative with respect to p. Equation (2.9) is the analog of the finite-differences relation (7) of Ref. [17]. Upon integration, and recalling Eq. (2.3), one obtains

$$\tau_p = \frac{t_+}{1-\gamma}(1-\gamma^p) - t_+ p, \tag{2.10}$$

where $\gamma = e^{-b}$. Notice that an additional assumption made in [17] about the codimension of the set of points supporting the most intense events in a turbulent flow is not necessary in the present derivation. In fact, SL's and CC's formulas (2.4) and (2.5), are recovered by the positions $(t_+, \gamma) = (2/3, 2/3)$ and $(t_+, \gamma) = (1, 1+\tau_2)$, respectively.

In order to treat the region $p < 0$, in such a way that no exponential divergence occurs, it is necessary to allow for a change of sign before the first derivative of τ_p in Eq. (2.9). Moreover, we make a linearity assumption for τ_p in the limit $p \to -\infty$ [7]: in fact, in such a limit, $\langle \varepsilon^p(\ell) \rangle \to \varepsilon_{\min}^p(\ell)$, where $\varepsilon_{\min}$ is the minimum value assumed by $\varepsilon(\ell)$, and Eq. (1.5) implies that $\tau_p \sim t_- p$, for some t_-. Hence, in analogy with Eq. (2.7), we assume

$$Z_\ell(-\infty+h,-\infty) \sim \ell^{t_- h}. \tag{2.11}$$

We further interpolate between the two asymptotes $t_- p$ and $-t_+ p$ by introducing a function $f(p)$ with the following properties:

$$\lim_{p\to-\infty} f(p) = -1,$$
$$f'(p) \geqslant 0, \quad f''(a) = 0, \quad -\infty < a < +\infty, \tag{2.12}$$
$$\lim_{p\to+\infty} f(p) = +1,$$

i.e., the function has two horizontal asymptotes and an inflection point at $p=a$: three examples are shown in Fig. 1. Accordingly, we modify Eq. (2.8) to

$$\tau_{p+h}-\tau_p \approx -\frac{bh^2}{2}\{t_-[1-f(p)]+t_+[1+f(p)]\} +[1-bhg(p)](\tau_p-\tau_{p-h}), \qquad (2.13)$$

where the first term on the RHS accounts for the switch between the contributions of the two asymptotes and the function $g(p)$ in the second term on the rhs satisfies the same conditions as $f(p)$, so that the sign in front of τ_p' changes upon variation of p: this ensures that no exponential divergence occurs for $p\to-\infty$.

The continuous limit, $h\to 0$, now yields

$$\tau_p'' \approx -bg(p)\tau_p' - b[S+Df(p)], \qquad (2.14)$$

where $S=(t_+ + t_-)/2$ and $D=(t_+ - t_-)/2$. For simplicity, we pose $f(p)=g(p)$ in the following. For $p \gg 1$, Eq. (2.14) reduces to Eq. (2.9). The asymptotic limits $|p|\to\infty$ are easily verified: setting $\lim_{|p|\to\infty}\tau_p''=0$, in fact, yields $\tau_p'\to -t_+$, for $p\to+\infty$, and $\tau_p'\to t_-$, for $p\to-\infty$.

Equation (2.14) defines a class of models (more precisely, fit functions τ_p), one for each choice of the functions $f(p)$ and $g(p)$, which depend on four parameters: b, which weighs the relative importance of the asymptotic values of $Z_{\ell}(p+h,p)$ with respect to the current one [see Eq. (2.6)] and is the counterpart of β in Eq. (2.2), the asymptotic slopes t_+ and t_-, and the value $p=a$ at which the function $f(p)$ [and $g(p)$] has the inflection point. Of course, both $f(p)$ and $g(p)$ might contain more parameters: in the following, however, we shall constrain ourselves to elementary functions which satisfy conditions (2.12), with the further simplification $f(a)=0$.

The simplest choice for analytical calculations is $f(p)=g(p)=2H(p-a)-1$, where $H(x)$ is the Heaviside step function [20]. Upon substitution, Eq. (2.14) reads

$$\tau_p''=\begin{cases} b\tau_p'-bt_- & \text{for } p<a,\\ -\quad b\tau_p'-bt_+ & \text{for } p>a. \end{cases} \qquad (2.15)$$

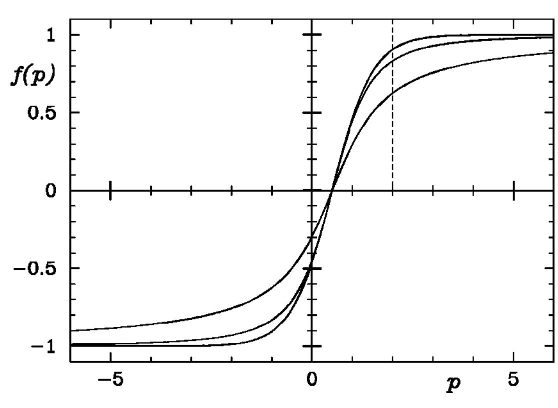

FIG. 1. Three of the sigmoidal functions $f(p)$ vs p employed in the computation of τ_p: at $p=2$ (indicated by the vertical dashed line) these functions are, from top to bottom, tanh($p-a$), $(p-a)/\sqrt{1+(p-a)^2}$, and 2 arctan$(p-a)/\pi$, with $a=0.5$.

A first integration yields

$$\tau_p'=\begin{cases} A_-e^{bp}+t_- & \text{for } p<a,\\ A_+e^{-bp}-t_+ & \text{for } p>a, \end{cases} \qquad (2.16)$$

where A_- and A_+ are constants. A second integration finally yields the ''biasymptotic'' formula

$$\tau_p=\begin{cases} \frac{A_-}{b}e^{bp}+t_-p+B_- & \text{for } p<a,\\ -\frac{A_+}{b}e^{-bp}-t_+p+B_+ & \text{for } p>a, \end{cases} \qquad (2.17)$$

which contains the two further constants B_- and B_+. The values of $A_\pm$ and $B_\pm$ can be fixed by imposing the continuity of τ_p' and τ_p at $p=a$ and recalling relations (2.3):

$$A_-e^{ab}+t_-=A_+e^{-ab}-t_+,$$

$$\frac{A_-}{b}e^{ab}+at_-+B_-=-\frac{A_+}{b}e^{-ab}-at_++B_+,$$

$$\frac{A_-}{b}+B_-=0,$$

$$-\frac{A_+}{b}e^{-b}-t_++B_+=0.$$

III. COMPARISON WITH THE EXPERIMENT

The test function τ_p of Eq. (2.17) contains four unknown parameters (a, b, t_-, and t_+), the meaning of which is quite clear: a determines the position of the maximum of τ_p, b the speed of the crossover from a parabolic shape around $p=a$ [as in the K62 equation (1.7)] to a straight line behavior for $|p|\to\infty$, and t_- and t_+ are the asymptotic slopes.

Lack of physical insight in the mechanisms of turbulence makes an estimation of these parameters utterly difficult. So far, not even the value $a\approx 0.5$ has been explained: to our knowledge, the question itself of the position of the maximum of τ_p has never been posed. Similarly, the portion of the curve τ_p vs p for $p<0$ has not been studied until recently [7]: therefore, no guess exists about the value of t_-. Vice versa, at least two proposals exist for t_+, as discussed above in connection with equations (2.4) and (2.5). Finally, the value of b is the least likely to be fixed by straightforward physical considerations, since it depends on the form of the function $f(p)$ used to interpolate between the asymptotic limits $p\to\pm\infty$.

In fact, comparison with the experimental data shows that a broad class of functions $f(p)$ yields equally accurate fits (of course, for different parameter values). This should not be surprising since even the step function provides good results, notwithstanding its discontinuity. In addition to $2H(p-a)-1$, we have tested the following functions (we pose $x=p-a$, for simplicity): sgn$(x)[1-e^{-|x|}]$, tanh(x), $x/\sqrt{1+x^2}$, and $2\arctan(x)/\pi$.

The curve τ_p vs p from Eq. (2.17) that best fits the experimental data is shown in Fig. 2: the length of the error

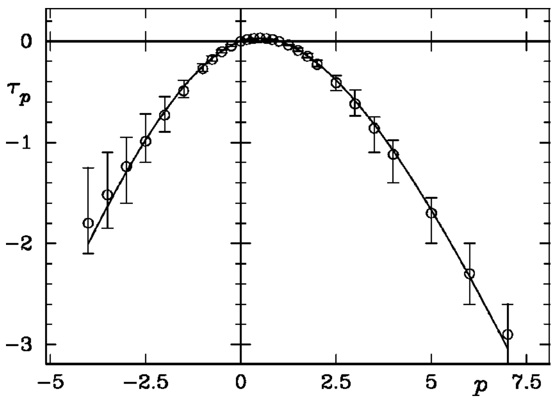

FIG. 2. Values of τ_p vs p, estimated from various atmospheric time series, compared with the best fitting curve obtained from Eq. (2.17). The length of the error bars has been used as a weight in a Marquardt-Levenberg least-square algorithm.

bars, estimated from comparison among various atmospheric time series [7], was used as a weight for the data points. The resulting parameter values are $a=0.475$, $b=0.278$, $t_-=1.06$, and $t_+=0.873$. While a is indistinguishable from 0.5, within the resolution allowed for by the statistical errors, the other three values are close to those of the CC formula (2.5). This, in fact, predicts $b=-\ln\gamma=-\ln(1+\tau_2)\approx 0.25$ [see Eq. (2.10)], and assumes $t_-=t_+=1$. A similar fit, made with uniform weights, however yields $a=0.488$, $b=0.468$, $t_-=0.717$, and $t_+=0.656$: that is, values much closer to the SL formula (2.4) (for which $b=0.406$ and $t_-=t_+=2/3$).

The range in which p has been varied has been confined to $[-4,7]$ in order to avoid fitting highly unreliable data points: below $p=-4$, signal discretization and instrumental noise are the main hindrance to the analysis; above $p=7$ low statistics and, possibly, nonstationarity play a major role. Estimates made at high p values (e.g., $p>10$), as often reported in the literature, should be taken with skepticism. Notwithstanding these precautions and the good quality of our data (high Reynolds-Taylor number, resolution and sampling rates), the precision of the results is not sufficient to discriminate between different interpolating functions $f(p)$ or different models. For comparison, we mention that a good fit is obtained with $f(x)=2\arctan(x)/\pi$, $a=0.5$, $t_-=0.71$, $t_+=0.63$, and $b=0.38$. The biasymptotic formula Eq. (2.17), while showing a much better agreement with the data than SL's or CC's formulas, which diverge exponentially for $p\to-\infty$, does not definitely turn the scale in favor of either contender.

In Fig. 3, we display the differences between the estimated values of τ_p and the two best-fit functions described above (with uniform and nonuniform weights). The weighted fit (open circles) is closer to the experiment for $0<p<2$ but more distant for $p<-3$ and $p>6$ [as already remarked, it yields a curve close to Eq. (2.5) which has similar features]. It must be noticed that these fits are made over all values of p and not only for $p>0$, which is the range of ''validity'' of the ''one-sided'' SL-CC approaches.

These results show, once more, that the question of the asymptotic behavior of τ_p for $|p|\to\infty$ can hardly be settled from experimental data [19], unless considerably better estimators of τ_p are found. An improved scaling relation, which accounts for deviations of the moments (1.5) from power-

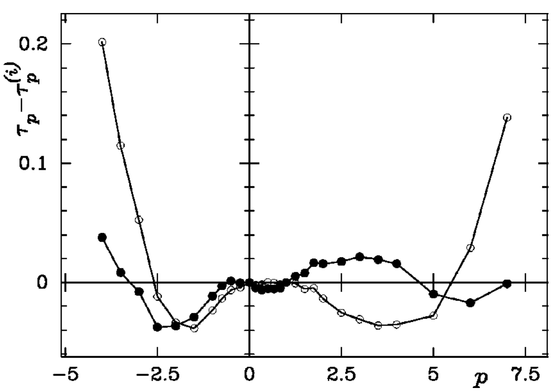

FIG. 3. Difference between the curve τ_p vs p, estimated as in Fig. (2), and the best fitting curves $\tau_p^{(i)}$ obtained from Eq. (2.17) using the error bar lengths as weights ($i=1$, open circles) and no weights at all ($i=2$, solid circles).

law behavior is currently under investigation. Also, corrections to scaling arising from the influence of large-scale fluctuations [21] could be profitably applied.

Finally, in order to test the symmetry of the curve τ_p vs p around $p=1/2$, we have postulated the extended scaling relation

$$M_p \sim M_{1-p}^{a_p}, \tag{3.1}$$

where M_p is defined in Eq. (1.5) and $a_p=\tau_p/\tau_{1-p}$ is a new exponent to be estimated directly from Eq. (3.1). Asymmetry is, hence, characterized by the deviation of a_p from 1. The results, reported in Fig. 4, confirm a definite asymmetry which cannot be easily detected from inspection of Fig. 2 but which is clearly revealed by the fits made with the biasymptotic formula (2.17).

IV. CONCLUSIONS

We have introduced a family of differential models for the scaling exponent of the energy dissipation rate in turbulence. They are characterized by sigmoidal functions and require physical input for (at least) four different parameters. Comparison with the experiment shows that good results can be obtained with quite a broad choice of values, both for positive- and negative-order energy dissipation moments.

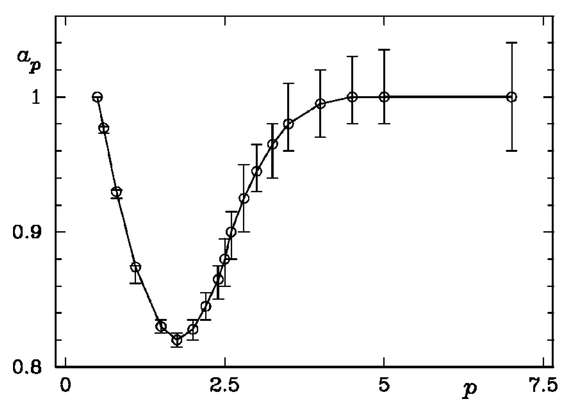

FIG. 4. ''Symmetry'' exponent $a_p=\tau_p/\tau_{1-p}$ vs p, estimated from Eq. (3.1) for the same data as in Fig. 2. The smallest value of p considered is 0.5, where $a_p=1$.

Therefore, we confirm the difficulty of fixing such parameters by experiment only.

Hints for a physical modeling, however, can be obtained from the differential equations. Indeed, the choice of a constant function $f(p)$ for positive p [17,18] corresponds to an assumption of log-Poissonian statistics for the energy cascade [22]. Analogously, models defined by other functions $f(p)$ can be traced back to different statistical mechanisms which would be interesting to test in a direct way. Investigations in this direction are progressing.

ACKNOWLEDGMENTS

We gratefully acknowledge the receipt of data from M. Furger, J. Peinke, and R.O. Weber.

[1] A.N. Kolmogorov, Dokl. Akad. Nauk SSSR **30**, 301 (1941).
[2] A.S. Monin and A.M. Yaglom, *Statistical Fluid Mechanics* (MIT Press, Cambridge, MA, 1971), Vol. 1; *ibid.*, Vol. 2.
[3] A.N. Kolmogorov, J. Fluid Mech. **13**, 82 (1962).
[4] A.M. Obukhov, J. Fluid Mech. **13**, 77 (1962).
[5] F. Anselmet, Y. Gagne, E.J. Hopfinger, and R. Antonia, J. Fluid Mech. **140**, 63 (1984).
[6] A. Arneodo *et al.*, Europhys. Lett. **34**, 411 (1996).
[7] R. Badii and P. Talkner, Phys. Rev. E **59**, 6715 (1999).
[8] R. Badii and P. Talkner, Europhys. Lett. **43**, 284 (1998).
[9] B.B. Mandelbrot, *The Fractal Geometry of Nature* (Freeman, San Francisco, 1982).
[10] C. Meneveau and K.R. Sreenivasan, Phys. Rev. Lett. **59**, 1424 (1987).
[11] E.A. Novikov and R.W. Stewart, Izv. Akad. Nauk SSSR, Ser. Geogr. Geofiz. **3**, 245 (1964).
[12] B.B. Mandelbrot, J. Fluid Mech. **62**, 331 (1974).
[13] U. Frisch, P.L. Sulem, and M. Nelkin, J. Fluid Mech. **87**, 719 (1978).
[14] R. Benzi, G. Paladin, G. Parisi, and A. Vulpiani, J. Phys. A **17**, 3521 (1984).
[15] E.A. Novikov, Phys. Fluids A **2**, 814 (1990).
[16] E.A. Novikov, Phys. Rev. E **50**, 3303 (1994).
[17] Z.S. She and E. Lévêque, Phys. Rev. Lett. **72**, 336 (1994).
[18] S. Chen and N. Cao, Phys. Rev. E **52**, 5757 (1995).
[19] M. Nelkin, Phys. Rev. E **52**, 4610 (1995).
[20] Notice, however, that $H(x)$ does not formally satisfy the condition on the second derivative f'' in Eq. (2.12) because of its discontinuity.
[21] J.M. Tchéou, M.E. Brachet, F. Belin, P. Tabeling, and H. Willaime, Physica D **129**, 93 (1999).
[22] Z.S. She and E.C. Waymire, Phys. Rev. Lett. **74**, 262 (1995).